Analytical Expression of Reflection-Spectrum Envelope for Sampled Gratings

Xiaoying He, Yonglin Yu, Wen Liu, and Dexiu Huang

Wuhan National Laboratory for Optoelectronics, Huazhong University of Science and Technology, Wuhan, 430074, P.R.China
Xiaoying.He@gmail.com

Abstract

Analytical method is proposed for calculating the reflection-spectrum envelopes of various sampled gratings including apodized gratings and interleaved gratings. Compared to the transfer matrix method, it provides a simple and fast way to evaluate overall performances of reflection-spectrum envelope. Accuracy of those expressions has been verified with simulated results obtained by the transfer matrix method. Impacts of grating parameters on the reflection-spectrum envelope could be clearly explained by using this analytical method. The shape of reflection-spectrum envelope is attributed to the shape of sampling function. Results with Gaussian-apodized sampled gratings have given a good understanding of derivation of sidelobes on every reflection peak, which are attributed to the whole grating profile function.

Keywords: Sampled grating, Reflection-spectrum envelope, Fourier method, Apodized grating, Interleaved sampled grating

1 Introduction

Sampled gratings (SGs) are well recognized as critical components for optical communications and optical sensor systems because of their wide applications such as tunable semiconductor reflectors [1, 2], multi-channel dispersion compensators [3, 4], multi-channel multiplexers-demultiplexers [5], repetition rate multiplication [6], and so on. For all of these applications, multi-channel gratings with uniform reflection peaks are needed. Especially, the grating with multiple identical peaks, as tunable semiconductor reflectors, will significantly improve the performance of laser over a widely tuning range. Various kinds of design and writing techniques have been proposed for this purpose, including Sinc-apodization[7], multiple-phase shift technique [8], and interleaved technique[9]. However, the transfer matrix method can not convey the relation of grating parameters and top-flatness and width of reflection-spectrum envelope. Moreover, with the increment of total grating length the calculated time for simulation of transfer matrix method is too long. Therefore, it is necessary to propose analytical expressions of reflection-spectrum envelopes for various sampled gratings to study .impacts of grating parameters on reflection-spectrum envelopes.
In this paper, an analytic expression for reflection-spectrum envelope (RSE) is proposed and demonstrated, which can be used to analyze the flatness and 3dB envelope bandwidth of reflection-spectrum envelope (RSE) for various sampled gratings. Compared to the transfer matrix method, it provides a simple and fast way to evaluate overall performances of reflection-spectrum envelope. This method is very useful and can be employed in related domains.

2 Theory of reflection-spectrum envelope

2.1 Analytical expression by Fourier method

The main spectral features of sampled grating, whether photo-refractive grating or etched grating, can

be derived from the modulation of the effective refractive index. The effective refractive-index profile can be governed by:

$$n_{eff}(z) = n_{0.eff}(z) + \underline{\delta n}_{eff}(z) \cdot \left[f(z) * \left(\sum_{i=-\infty}^{\infty} \delta(z - iZ_0) \cdot g(z) \right) \right] \cdot \left\{ 1 + \upsilon \cos\left(\frac{2\pi}{\Lambda} z \right) \right\} \tag{1}$$

$$f(z) = \begin{cases} 1, & -\frac{Z_g}{2} \le z \le \frac{Z_g}{2} \\ 0, & otherwise \end{cases} \tag{2}$$

$$g(z) = \begin{cases} 1, & -\frac{L}{2} \le z \le \frac{L}{2} \\ 0, & otherwise \end{cases} \tag{3}$$

where $n_{0,eff}$ is the local mean value of the effective refractive index for the propagating mode, $\underline{\delta n}_{eff}$ is the *dc* index change spatially averaged over a grating, υ is the fringe visibility of the index change, Λ is the grating period, Z_0 and Z_g are the sampling period and the grating segment length in the sampling period, respectively. L is the total length of sampled grating. The rectangular function $f(z)$ is the sampling function of the SG without apodization, and the rectangular function $g(z)$ is the whole grating profile function without apodization related with the total length L of the SG. The coupling coefficient κ_0 is a constant related with $\underline{\delta n}_{eff}$ in single-mode uniform Bragg grating. Consequently, the coupling coefficient $\kappa(z)$ of the SG along the propagation axis z can be given by:

$$\kappa(z) = \kappa_0 \cdot f(z) * \left[\sum_{i=-\infty}^{\infty} \delta(z - iZ_0) \cdot g(z) \right]. \tag{4}$$

The coupling coefficient $\kappa(z)$ transformed by Fourier analysis is:

$$\mathrm{K}(\beta) = \kappa_0 \cdot Z_g \sin c\left(\frac{\beta Z_g}{2} \right) \cdot \left[N \sin c\left(\frac{\beta L}{2} \right) * \sum_{n=-\infty}^{\infty} \delta(\beta - n\beta_0) \right] \cdot \tag{5}$$

This equation indicates the relation of the coupling coefficient and the spatial frequency β, where N is the sampling number. β_0 and β can respectively be expressed by $2\pi/Z_0$ and $2n\pi/Z_0$. The coupling coefficient $\kappa(n)$ corresponding to the nth Fourier component in the SG is:

$$\kappa(n) = \kappa_0 \frac{Z_g}{Z_0} \sin c\left(\pi n Z_g / Z_0 \right) e^{i\pi n Z_g / Z_0} \ . \tag{6}$$

Due to the analogy between the sampled grating and the unsampled grating, the every peak power reflectivity calculated by the coupled-mode theory is approximately equal to:

$$R_p(n) = \tanh^2\left(\left| \kappa(n) \right| L \right). \tag{7}$$

The diffracted order n can be expressed as a function of the wavelengths λ:

$$n = \frac{Z_0}{\pi} \left(\frac{2n_{0,eff}\pi}{\lambda} - \frac{\pi}{\Lambda} \right) \tag{8}$$

where Z_0/π can be regarded as the diffracted numerical aperture of sampled grating, and $2n_{0,eff}\,\pi/\lambda$ is the wave number. As thus, substituting Eq.(8) into Eq.(6), and associating with Eq.(7), the analytical expression for the RSEs can be expressed by:

$$R_{env}(\lambda) = \tanh^2\left(\left| \kappa_0 \frac{Z_g}{Z_0} \sin c\left(\pi \frac{Z_g}{Z_0} \cdot Z_0 \left(\frac{2n_{0,eff}}{\lambda} - \frac{1}{\Lambda} \right) \right) e^{i\pi Z_g \left(\frac{2n_{0,eff}}{\lambda} - \frac{1}{\Lambda} \right)} \right| \cdot L \right). \tag{9}$$

The Sinc function in Eq.(9) is related with the Fourier transform component function of the rectangular function $f(z)$. From Eq.(9), it is clear that the shape of the RSEs is determined by the Sinc function related with the grating segment length Z_g, the local mean value of effective refractive index $n_{0,eff}$ and the grating period Λ. Clearly, only using Eq. (9), the basic performances of the RSEs can be

analyzed accurately, the optimal design of parameters for the SGs can be obtained as well. This will be helpful to design multi-channel gratings with a broad flat-top reflection spectrum.

2.2 Reflection-spectrum envelope of conventional sampled grating

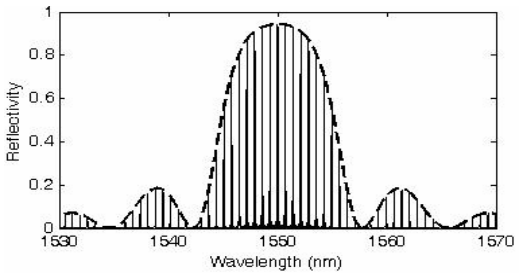

Fig.1 Reflection spectrum and reflection-spectrum envelope of conventional sample grating

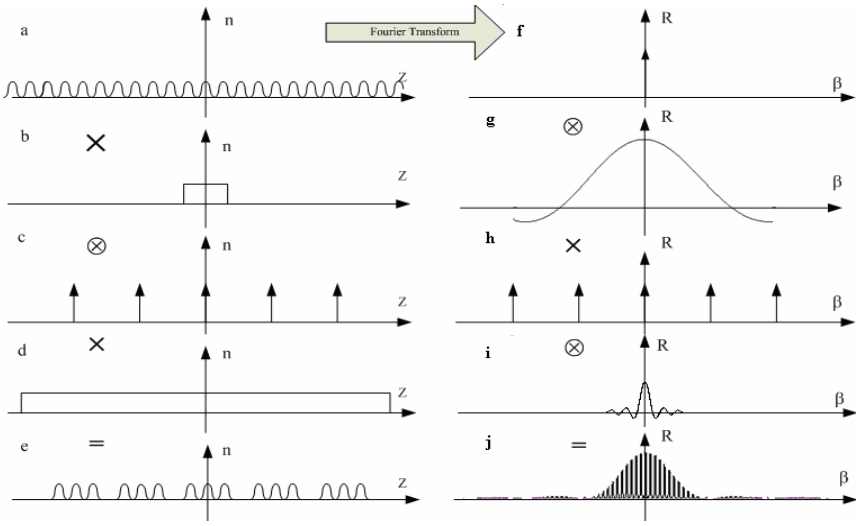

Fig.2 Conventional sampled grating in real space and spatial frequency β space

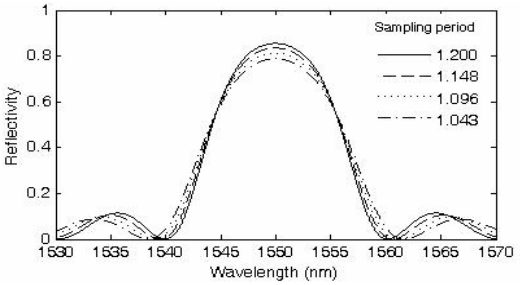

Fig.3 (a) Reflection-spectrum envelope of conventional sampled grating with different sampling period and the duty cycle Z_g/Z_0=1/15

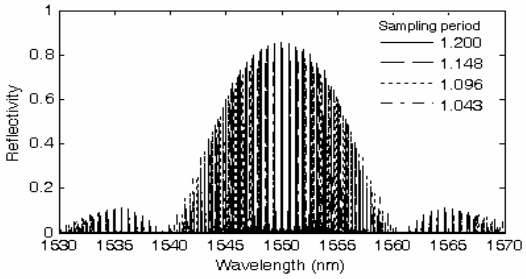

Fig.3 (b) Reflection spectrum of conventional sampled grating with different sampling period and the duty cycle Z_g/Z_0=1/15

The RSE of the conventional sampled grating calculated by the analytical expression Eq.(9) is plotted with the dashed line in Fig.1. The transfer matrix method is also used to verify the proposed method. Parameters are used here as follows: $n_{0,eff}$ =1.485, Λ=521.7nm, $\bar{\delta}n_{eff}$ =5×10^{-4}, and N=20 (the number of the sampling period). Simulation with the transfer matrix method is a time-consuming task especially for long gratings. Obviously the proposed method provides a simple and fast way to evaluate overall performances of SGs, such as the flatness and 3dB bandwidth of reflection-spectrum envelop. As shown in Fig.1, the calculated RSE are well consistent with the reflection-peak values in reflection spectrum obtained by the transfer matrix method. The spatial corrugation and reflection frequency spectrum of the conventional sampled grating have a relation analogous to the Fourier transform, which are illustrated in Fig.2. The spatial index profile of the sampled grating in Fig.2 (e) can be composed by the mathematic operation of the four spatial index profile functions in Fig.2(a), Fig.2(b), Fig.2(c), and Fig.2(d). The reflection spectrum corresponding to the spatial frequency β in Fig.2(j) consists of the four parts of Fig.2(f), Fig.2(g), Fig.2(h), and Fig.2(i). From Fig.2, it is apparent that the every reflection peak and its sidelobes are related with the Fourier transform component function of the rectangular function $g(z)$, and the rough shape of the RSEs is determined by the Fourier transform function of the rectangular function $f(z)$. Assuming that the conventional sampled grating has infinite length, their sidelobes will be eliminated and the linewidth of every reflectivity peak is quite narrow.

The impact of the sampling period on reflection spectrum envelope is calculated by the proposed method and the transfer matrix method respectively, and shown in Fig.3(a) and Fig.3(b). Obviously, Fig.3(a) presents a clear picture of dependence of reflection spectrum envelope on the sampling period. In Fig.3(a), Under the fixed duty cycle Z_g/Z_0 of 1/15, as the sampling period increases, the reflectivity in the 3dB envelope slightly increases.

3 Extended analysis to complex sampled gratings

3.1 Sampled Gaussian-apodized gratings

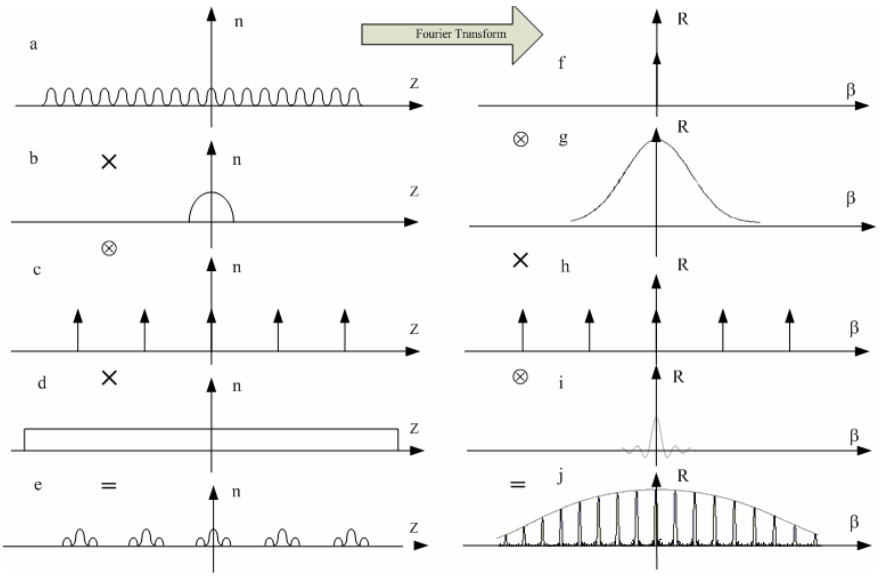

Fig.4 Sampled Gaussian apodized grating in real space and spatial frequency β space

In Fig.4(e) and Fig.5(b), the Gaussian-apodization is employed to the grating segment in per-sampling period, which is called the sampled Gaussian-apodized grating. It is shown in Fig.5(c) that the sidelobes have not been eliminated by the Gaussian-apodization on the sampling function, whereas the reflection-spectrum envelope of the sampled Gaussian-apodized grating presents a Gaussian-function

shape in Fig.5(a). Therefore, an apodized tailoring on the sampling function of the grating segment can change the shape of the reflection-spectrum envelope. The Gaussian-apodization function is:

$$G(z) = \exp\left[-\frac{10(z - Z_0/2)^2}{Z_0^2}\right]. \tag{10}$$

According to the Fourier method, the analytic expression of reflection-spectrum envelope on sampled Gaussian apodized grating is defined by:

$$R_{env}(\lambda) = \tanh^2\left(\left|\kappa_0 \frac{Z_g}{Z_0}\sqrt{\frac{\pi}{10}}\exp\left(-\frac{\pi}{40}\left(\frac{Z_g}{Z_0}\right)Z_0\left(\frac{2n_{0,eff}}{\lambda} - \frac{1}{\Lambda}\right)\right)e^{i\pi Z_g\left(\frac{2n_{0,eff}}{\lambda} - \frac{1}{\Lambda}\right)}\right| \cdot L\right). \tag{11}$$

Depending on Eq. (11), the calculated reflection-spectrum envelope is plotted with dashed line in Fig.5(a), which is in good agreement with the reflection-spectrum simulated by the transfer matrix method. The envelope shape is related with the Fourier function of the sampling function.

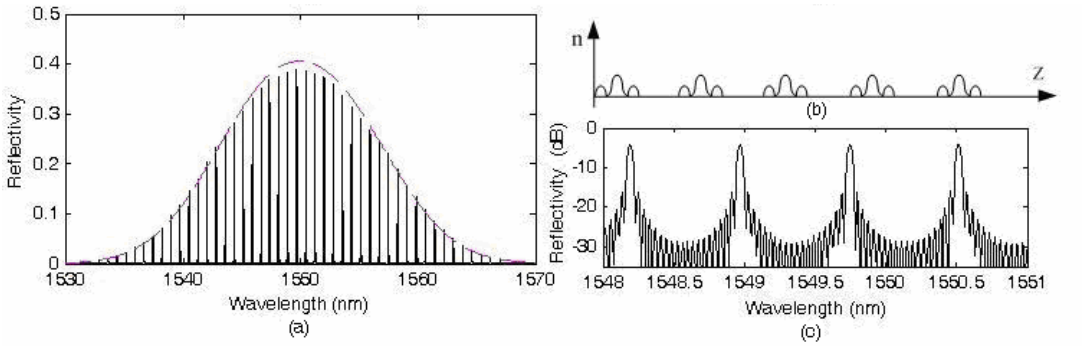

Fig.5 Reflection spectrum, reflection-spectrum envelope and spatial index profile of sampled Gaussian-apodized grating

3.2 Gaussian-apodized sampled gratings

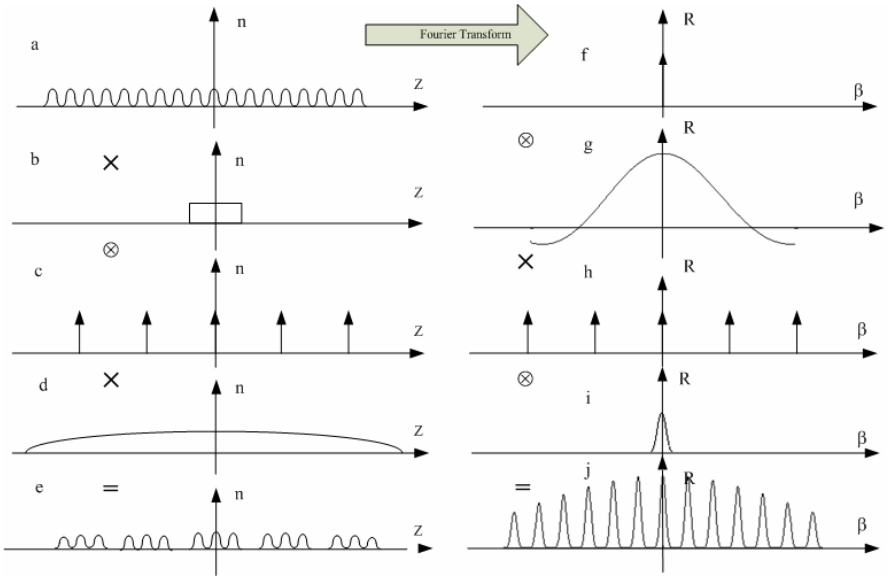

Fig.6 Gaussian-apodized sampled grating in real space and spatial frequency β space

Highly undesirable sidelobes can cause serious crosstalk between adjacent channels. In order to demonstrate that the sidelobes are derived from the Fourier transforms component function of the whole grating profile function, the Gaussian-apodization can be introduced into the whole grating

profile function, which is regarded as the Gaussian-apodized sampled grating and its index profile is shown in Fig.6(e) and Fig.7(b). The apodized tailoring on the grating can decrease the whole reflectivity of reflection spectrum both sampled Gaussian-apodized gratings and Gaussian-apodized sampled gratings. The shape of reflection-spectrum envelope for the Gaussian apodized sampled grating is Sinc shape, as shown in Fig.7(a) with dashed line. Compared Fig.5(c) with Fig.7(c), the sidelobes can completely eliminated by Gaussian apodization on the whole grating profile function. Example of Gaussian-apodized sampled gratings has provided a good understanding of sidelobes on every reflection peak, which are attributed to the whole grating profile function. Similar to the expression of sampled Gaussian-apodized gratings, the analytic expression of reflection-spectrum envelope on Gaussian-apodized sampled gratings is defined by:

$$R_{env}(\lambda) = \tanh^2\left(\left|\kappa_0 \frac{Z_g}{Z_0}\sqrt{\frac{\pi}{10}}\sin c\left(\pi \frac{Z_g}{Z_0}\cdot Z_0\left(\frac{2n_{eff}}{\lambda}-\frac{1}{\Lambda}\right)\right)e^{i\pi Z_g\left(\frac{2n_{eff}}{\lambda}-\frac{1}{\Lambda}\right)}\right|\cdot L\right). \quad (12)$$

By Eq. (12), the reflection spectrum envelope is calculated as shown in Fig.7(a) (dashed line), and the inside reflection spectrum is obtained by the transfer matrix method (solid line).

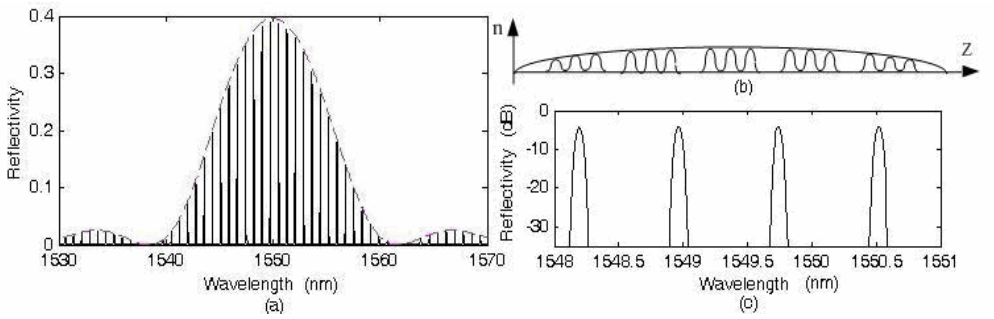

Fig.7 Reflection spectrum, reflection-spectrum envelope and spatial index profile of Gaussian-apodized sampled grating

3.3 Interleaved sampled gratings with phase shift

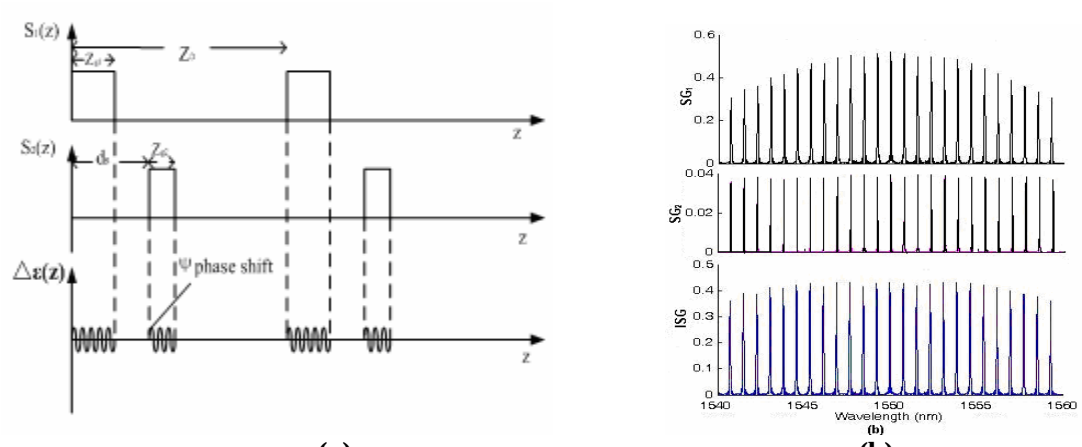

(a) **(b)**

Fig.8 Structure and mechanism of the ISG with ψ phase shift.
(a) sample functions S1(z), S2(z) and resulting index profile △ε(z) of the ISG with ψ phase shift;
(b) mechanism of the ISG with ψ=π phase shift.

Structure and mechanism of the interleaved sampled gratings (ISGs) with ψ phase shift are schematized in Fig.8. The sampling function $S_1(z)$ of the first sampled grating (SG_1) is shown in Fig.8(a). The second sampled grating (SG_2) with the sampling function $S_2(z)$ has a ψ phase shift at each grating burst. The sampling period Z_0 of the SG_1 is the same as that of the SG_2 as shown in

Fig.8(a). The grating segment lengths of the SG_1 and the SG_2 are, respectively, Zg_1 and Z_{g2}. The interleaved length *ds* is the length between the grating burst of the SG_1 and the grating burst of the SG_2 in each sampling period. The second sampled grating, the SG_2, is interleaved into the SG_1. The flat reflectivity spectrum of the ISG with a π phase shift illuminated in Fig.8 (b) is given by summing amplitude and phase of the field reflectivity of two sampled gratings. The second sampled gratings with a phase shift can provide a modification of reflection-spectrum envelope of the SG_1. The analytical expression for reflection-spectrum envelope of ISG_ψ can be estimated for lossless gratings by:

$$R_{env}(\lambda)=\tanh^2\left[\left|\kappa_0\left[\frac{Z_{g1}}{Z_0}\sin c\left(\pi Z_{g1}\left(\frac{2n_{rff}}{\lambda}-\frac{1}{\Lambda}\right)\right)\exp\left(i\pi Z_{g1}\left(\frac{2n_{rff}}{\lambda}-\frac{1}{\Lambda}\right)\right)\right.\right.\right.$$
$$\left.\left.\left.+\exp(-i\psi)\cdot\frac{Z_{g2}}{Z_0}\sin c\left(\pi Z_{g2}\left(\frac{2n_{rff}}{\lambda}-\frac{1}{\Lambda}\right)\right)\exp\left(i\pi\left(Z_{g2}+2d_s\right)\cdot\left(\frac{2n_{rff}}{\lambda}-\frac{1}{\Lambda}\right)\right)\right]\right|\cdot L\right]. \quad (13)$$

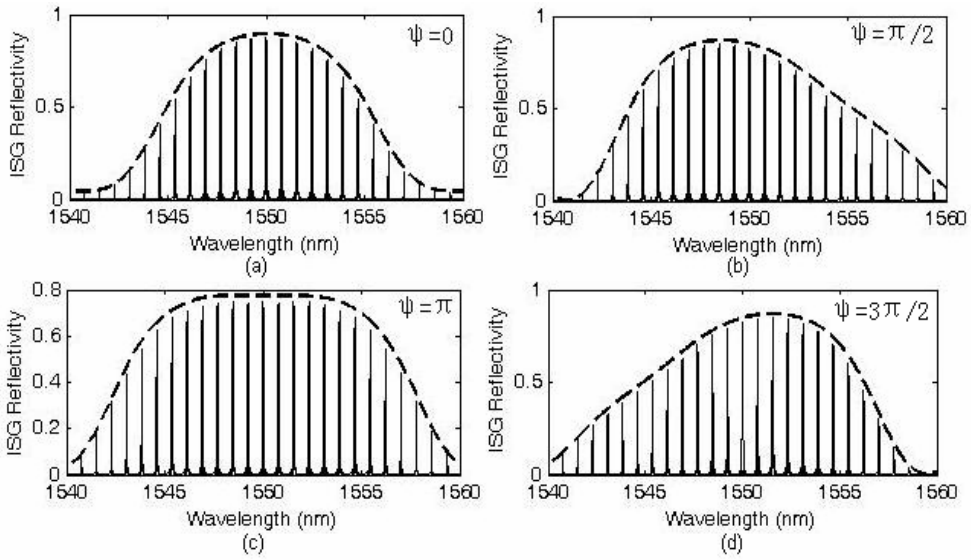

Fig.9 Reflectivity and reflection-spectrum envelopes of the ISGs with phase shifts of ψ=0, π/2, π, and 3π/2

In Fig.9, the peak reflectivity of the SG_1 has been modified by the reflectivity of the SG_2 with the ψ phase shift, which leads to the ISG_ψ with different reflection-spectrum envelopes. From Fig.9, the field reflection spectrum envelopes of the SG_2 with ψ=π/2 and ψ=3π/2, respectively, have a blue shift and a red shift of reflection-spectrum envelope top. Originated from Eq. (13), the phase shifts can be introduced into the filed reflectivity of the SG_2 to modify the coupling coefficient κ_n of the SG_1. An overturn occurs within the coupling coefficient κ_n between the SG_2 with ψ=π phase shift and the SG_2 with ψ=0 phase shift, as well as the filed reflectivity in Fig.9. For the same spectral window, the ISG with the π phase shift provides the flattest top envelope of the ISGs with phase shifts. As shown in Fig.9, accuracy of analytical expression on reflection spectrum envelope (dotted lines) is verified by calculated results (dashed lines) in good agreement with the peak reflectivity spectra (solid lines) obtained by the transform matrix method.

4 Conclusion

Analytical expressions of reflection-spectrum envelope for various complex sampled grating are derived by the Fourier theory in detail. It has been shown that this analytical method can be extended to analyze the reflection-spectrum envelopes of some complex SGs, such as the Gaussian-apodized sampled gratings, sampled Gaussian-apodized gratings, and interleaved sampled gratings with phase shift. Compared to the transfer matrix method, it provides a simple and fast way to evaluate overall performances of reflection-spectrum envelope for sampled gratings. Accuracy of those expressions has

been verified by a good agreement of calculated results with the simulated reflectivity spectrum obtained by the transfer matrix method. It is clarified that those sidelobes on every reflection peak are derived from the Fourier transform component function of the whole grating profile function. The shape of reflection-spectrum envelope is governed by the Fourier transform function of the sampling function.

Acknowledgements

The authors undertook this work with the supports of the National Natural Science Foundation of China under Grant No. 60677024, the National High Technology Research Development Program of China under Grant No. 2006AA0320427.

References

[1] Jayraman, V. (1993). Theory, design, and performance of extended tuning range semiconductor laser with sampled gratings. *IEEE J. Quantum Electron.,* 29:1824-1834.
[2] He, X. (2006). Theoretical analysis of widely tunable external cavity semiconductor laser with sampled fiber grating. *Optic. Commun.,* 267:440-446.
[3] Chen, X. F. (2000). Analytical expression of sampled Bragg gratings with chirp in the sampling period and its application in dispersion management design in a WDM system. *IEEE Photon.Technol.Lett.,* 12:1013-1015.
[4] Dai, Y. (2006). Dispersion compensation based on sampled fiber Bragg gratings fabricated with reconstruction equivalent-chip method. *IEEE Photon, Technol. Lett.,* 18:941-943.
[5] Loh, W. H. (1999). Novel designs for sampled grating based multiplexers-demultiplexers. *Opt.Lett.,* 24:1457-1459.
[6] Petropoulos, P. (2000). Generation of a 40 GHZ pulse stream by pulse multiplication with a sampled fiber Bragg grating. *Opt. Lett.,* 25:521–523.
[7] Ibsen, M. (1998). Sinc-sampled fiber Bragg gratings for identical multiple wavelength operation. *IEEE Photon, Technol. Lett.,* 10:842-845.
[8] Ishii,H. (1993). Multiple-phase-shift super structure grating DBR lasers for broad wavelength tuning. *IEEE Photon.Technol. Lett.,* 5:613-615.
[9] Gioannini, M. (2001). Novel interleaved sampled grating mirrors for widely tunable DBR laser. *IEE Proceedings,* 148:13-18.